

Proceedings of International Collaboration on Advanced Neutron Sources (ICANS-VII), 1983 September 13-16
Atomic Energy of Canada Limited, Report AECL-8488

ASPUN, ARGONNE SUPER INTENSE PULSED SPALLATION NEUTRON SOURCE

T. K. Khoe and R. L. Kustom
Physics Division
Argonne National Laboratory
9700 S. Cass Ave.
Argonne, IL 60439

Introduction

Argonne has been in the process of developing plans for pulsed spallation neutron source facilities that would extend the flux levels by at least an order of magnitude over fluxes provided by facilities that are either now in operation or in construction. The ANL facility is called ASPUN for Argonne Super Intense Pulsed Spallation Neutron Source. The heart of ASPUN is a Fixed-Field Alternating Gradient (FFAG) proton synchrotron which, in our opinion, has great potential as a driver for a spallation neutron source.

The FFAG synchrotron was extensively studied in the 1950's and early 1960's at the Midwestern Universities Research Association (MURA) laboratories in Stoughton, Wisconsin.¹ An FFAG accelerator has dc excited magnetic fields into which beam is injected on the inside radius and as the beam is accelerated, the average equilibrium orbit radius grows. Frequency modulated rf cavities are used to accelerate the beam with a voltage and frequency program that tracks the beam energy.

The early FFAG accelerators were studied for use as high energy particle accelerators, a role which required a large momentum change from injection to extraction. The transverse focussing of the beam in an FFAG accelerator is accomplished through a combination of the entrance and exit edge angles and a field gradient from the inner radius to the outer radius of the machine. To achieve constant edge angles, the magnets spiral radially outwards, which for the early FFAG accelerators was quite extensive because of the large momentum difference between injection and extraction. However, the momentum range for use of an FFAG accelerator as a proton driver in a spallation source is about 2.5-2.7. Thus, the radial extent of the magnet is quite nominal, leading to a relatively simple FFAG accelerator design.

A discussion of the relative merits and potential of the FFAG driver is presented in Section III.

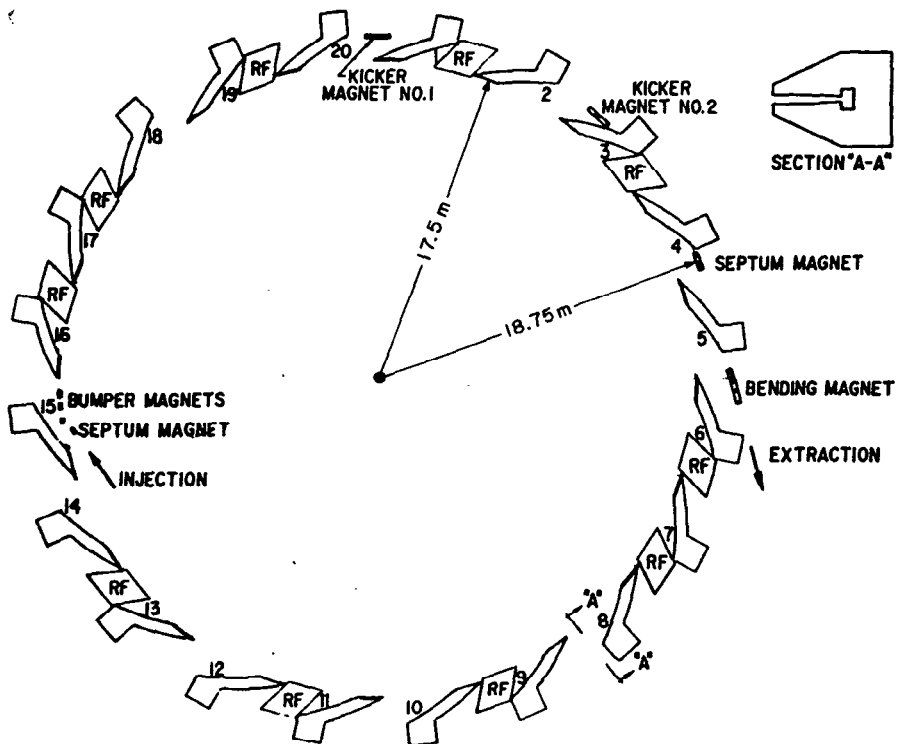


Fig. 1. Schematic view of FFAG ring.

Fixed-Field Alternating Gradient (FFAG) Design

The design is based on 200 MeV H^- to H^+ stripping injection. The extraction energy is 1100 MeV and the repetition rate without beam stacking is 220 Hz. The linac must provide 32 mA of H^- beam for 500 μ sec at the 220 Hz repetition rate. The duty factor of the linac must be somewhat greater than 11% to allow for rf filling and stabilization before beam injection.

A schematic view of the FFAG ring is shown in Figure 1. Table 1 gives the machine parameters. The injection radius is 17.5 m. The injection system is shown in Figure 2. The normal equilibrium orbit is the dashed line shown in Figure 2. The four bump magnets, B_1 , B_2 , B_2' , and B_1' , deflect the equilibrium orbit along the dot-dash line through the stripper foil at point S. The 200 MeV H^- beam enters through the septum magnet, SM. The B' magnets operate with a maximum field of 0.39T and are 25 cm long and the B magnets operate with a maximum field of 0.54T and are 37.5 cm long. The septum magnet operates at 0.6T and is 60 cm long. The horizontal phase-plane ellipse for 700 μ m-mrad emittance at the stripper foil is shown in Figure 3. The bumper and septum magnet fields decrease so that the stripper foil effectively appears to start at $(x, x') = (0, 0)$ and then moves inward along the negative major axis. Proper control of the decrease in field will produce uniform charge distribution in horizontal space leading to a smaller space charge effect. Magnets in the injection line will be used to distribute the beam uniformly in vertical phase space.

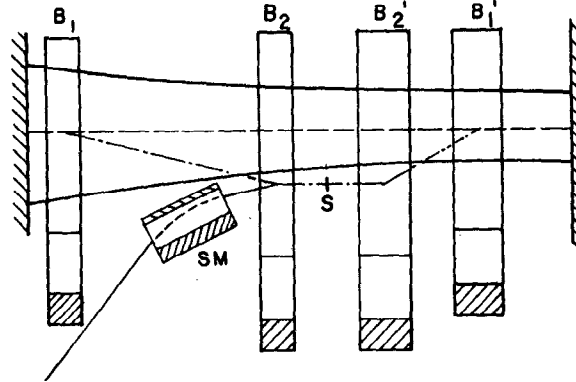


Fig. 2. Injection system showing four bumper magnets, septum magnet, and stripper foil.

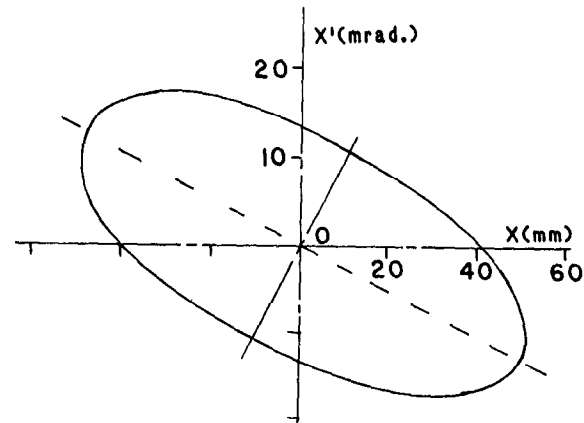


Fig. 3. Horizontal phase plane ellipse at stripper foil for 700 μ m-mrad emittance.

Table 1. Machine parameters

Injection energy (MeV)	200
Extraction energy (MeV)	1100
Injection radius (m)	17.5
Extraction radius (m)	18.75
Injection field (T)	0.489
Extraction field (T)	1.281
Number of sectors	20
Angular width of sectors (deg)	4.5
Field index k	14
Spiral angle ζ (deg)	65
Radial betatron frequency ν_x	4.25
Vertical betatron frequency ν_z	3.25
Space charge limit	10^{14}
Beam emittance at 200 MeV	
Radial (mm-mrad)	π 700
Vertical (mm-mrad)	π 500
Peak rf voltage per cavity (kV)	30
Frequency range (MHz)	1.5-2.259
Harmonic number	1
Number of cavities	10
Average current (mA)	≈ 3.5
Repetition rate (pulses/second)	≈ 220
Beam bucket area (eV-sec)	4.15
Output energy spread (MeV)	± 19.5
Output bunch length (nsec)	136
Weight of sector magnet (ton)	
Pole and yoke	68
Coils	2.5
Power loss per sector magnet (kW)	140

The energy of the linac beam will be modulated to give a coasting beam energy spread of ± 3.2 MeV.

Adiabatic capture is accomplished by instantaneously exciting the rf cavities at 27 kV and linearly increasing the voltage to 150 kV in 150 μ sec.

The guide field in an FFAG accelerator is given by

$$B = B_0 \left(\frac{R}{R_0} \right)^k \left[1 + \sum_{n=1}^{\infty} f_n \cos nN(\theta - \tan \xi \frac{1}{n} R/R_0) \right] \quad (1)$$

where R is the radial distance from the machine center, $k = (R/B)(dB/dR)$ is the mean field index, θ is the azimuthal angle, f_n is the harmonic

component of the azimuthally varying field, N is the number of identical magnets, and ξ is the spiral angle. There are 20 magnets each with an angular width of 4.5° and a nearly sharp edge field so that the effective flutter, $(\sum f_p^2)^{1/2}$, is large. The pole of the magnet extends from $R=17.4$ m to 18.9 m. The magnet gap is constant from 17.5 to 18.0 m. The required field gradient in this region is supplied by pole face windings. The magnet gap is 220 mm, chosen to allow for 143 mm of peak to peak betatron amplitude, 20 mm of orbit error due to field errors and misalignment, 20 mm for pole face windings, 20 mm for the vacuum chamber wall, and 17 mm extra. The magnet gap decreases from 220 mm at a radius of 18.0 m to 111 mm at a radius of 18.9 m. The decrease is tailored to achieve the correct magnet gradient required by eq. (1). The magnet field at the injection radius of 17.5 m is 0.489 T and at the extraction radius of 18.75 m is 1.28 T. The magnet parameters are listed in Table 2.

The magnet will be designed to maintain the same flutter throughout the momentum range so that the betatron frequencies are independent of momentum. The values for the β and η functions for one period from straight section center to straight section center are shown in Figure 4 and the beam envelopes at injection with $\epsilon_x = 700$ mm-mrad and $\epsilon_y = 500$ mm-mrad are shown in Figure 5.

Table 2. Magnet Characteristics

Width of sector	4.5°
Minimum pole radius	17.4 m
Maximum pole radius	18.9 m
Spiral angle	65°
Main coil ampere turns	9.7×10^4 A
Pole face windings ampere turns	5.9×10^4 A
Weight of yoke and poles	68 tons
Weight of coils	2.5 tons
Power loss	~ 140 kW
Magnet height	2.5 m
Radial width	2.8 m

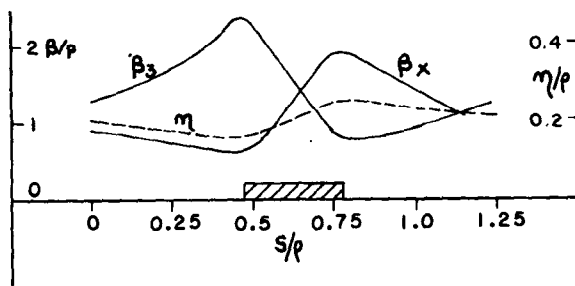


Fig. 4. β and η functions for one period starting at the center of a straight section.

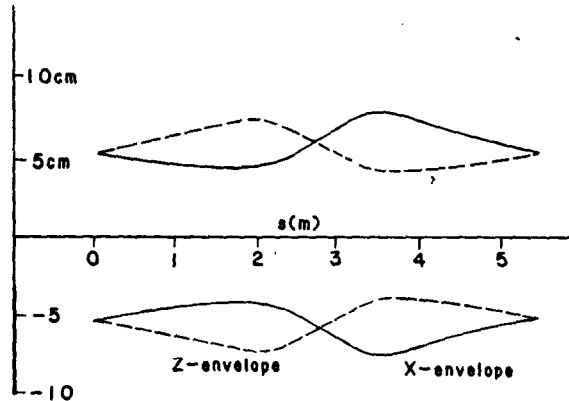


Fig. 5. Horizontal and vertical beam envelopes at injection for $\epsilon_x = 700$ mm-mrad and $\epsilon_y = 500$ mm-mrad.

The coherent space charge limit shortly after injection and bunching is 10^{14} ppp under the assumptions that the bunching factor is 0.45 , the transverse charge distribution factor is 1.35 , and the tune shift $\Delta v_z = 0.25$. The additional increase in space charge limit due to the momentum spread is not included, providing some additional margin of safety. The rf voltage and frequency are initially programmed to maintain the product $B_f \beta \gamma^2 > 0.375$, where B_f is the bunching factor, and β and γ are the velocity in units of light velocity and the energy in units of rest energy, respectively. Later in the cycle when space charge is not a consideration, the voltage and frequency are programmed to achieve maximum practical energy gain per turn. The rf voltage and frequency as a function of time is shown in Figure 6. The acceleration voltage is provided by ten cavities spaced around the machine. The frequency varies from 1.5 MHz at injection to 2.259 MHz at extraction. After the initial capture period, the rf voltage is increased from 150 kV to 300 kV in approximately 750 μ sec. The rf system parameters are listed in Table 3.

Table 3. Accelerating System Parameters

Number of cavities	10
Length of cavity	1.9 m
Cavity peak voltage	30 kV
Total volume of ferrite	11 m ³
Total peak ferrite losses	1.25 MW
Total peak beam power	6.48 MW
Cavity shunt resistance	7200 Ω
Coupling coefficient	6.2
Ferrite v_Δ injection	26.8
v_Δ extraction	12.5
Average rf flux density	0.0120 T
Maximum rf flux density	0.0145 T
D.C. biased H_{DC} (injection)	900 A/m
(extraction)	1800 A/m
Maximum H_{rf}	530 A/m ³
Power density in ferrite	114 kW/m ³

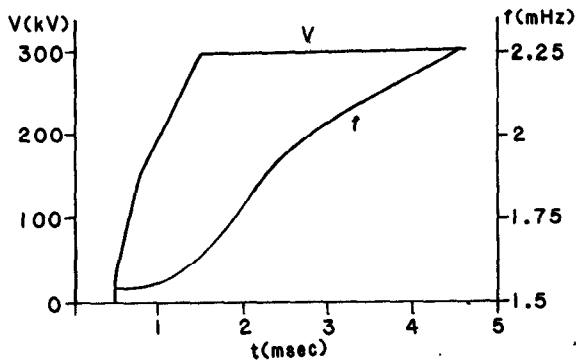


Fig. 6. Rf voltage and frequency as a function of time.

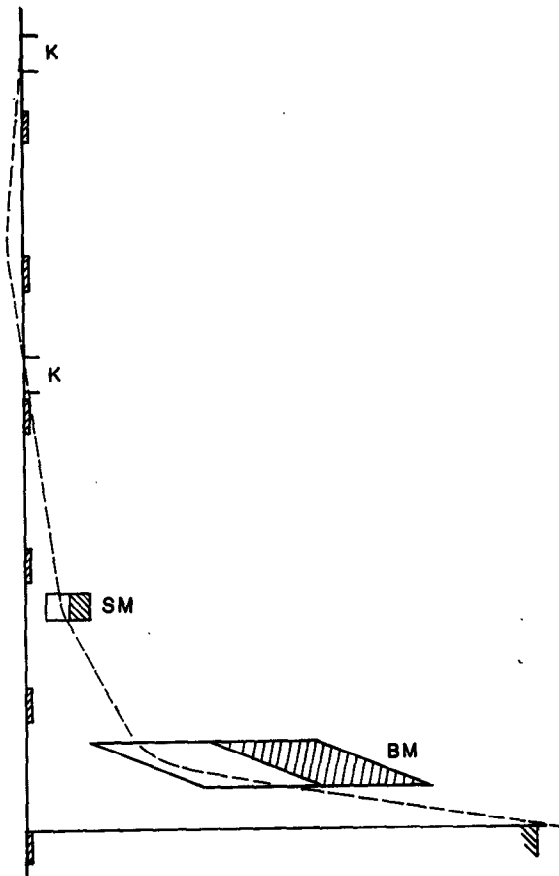


Fig. 7. The schematic plan view of the extraction system consisting of two fast ferrite kicker magnets, a thin septum magnet and a bending magnet.

Extraction is accomplished in one turn with two fast ferrite kicker magnets and a thin septum extraction magnet and a final bending magnet. A plan view of the extraction system is shown in Figure 7. The first fast kicker is located in

straight section 20. The magnet provides an inward kick of 10.34 mrad. This produces a coherent betatron oscillation of the beam bunch. The location of the second kicker in straight section 2 is 180° in betatron phase from the first kicker. The second kicker produces a 10.34 mrad outward kick which adds to the deflection angle produced by first kicker. Each of the kickers is 1.0 m long and operates at 0.0625T. The extraction septum magnet provides a 62.3 mrad deflection angle. It is 1 meter long and operates at 0.376T. The final extraction bending magnet is 2 meters long, operates at 1.4T, and provides a 460 mrad angular deflection.

Discussion

Several features of an FFAG accelerator suggest that this concept is well suited to use as an intense pulsed spallation source. The injection and capture in a dc magnetic field using charge exchange $H^- \rightarrow H^+$ injection has the potential for extremely high efficiency (~99%) since the rf voltage and frequency can be programmed with only that goal to achieve. The use of solid metal vacuum chambers provide very low impedances for beam instabilities, especially since the injection bumpers and extraction kickers are not seen by the beam beyond the immediate injection-extraction period. The energy gain per turn during acceleration can be made virtually constant so that most efficient use of the rf cavities is possible. More usable straight section space is available since the transverse focusing elements are contained totally within one magnet per lattice cell. The cost is much less than equivalent proton drivers.

Based on IPNS-I scaling, the peak neutron fluxes during the pulse would be 1.16×10^{17} n/cm²-sec. This flux would be almost 23 times more than the WNR-PSR facility at the Los Alamos National Laboratory and the SNS facility at the Rutherford-Appleton Laboratory based on equivalent scaling. The ASPUN facility would equal the proposed SNQ facility the KFA Laboratory, Jülich, Germany.

This conceptual design is adequately complete to satisfy proof-of-principle and encourage further development. Argonne proposes to build a mini-ASPUN FFAG that could be used to test the design of the magnet, the efficiency of capture and acceleration, and the stacking process. The machine would be added to the IPNS-I facility using the existing 50 MeV linac, transport lines and target. The mini-ASPUN FFAG would operate at 500 MeV, 100 μ a, and 30 Hz. This machine is described in some detail in the talk by G. H. Lander at this conference and so will not be described in further detail here.

References

1. F. T. Cole, et al., "Electron Model Fixed-Field Alternating Gradient Accelerator," Rev. Sci. Austr. 28, 403 (1957).